Specific heat of $CeRhIn_5$: Pressure-driven evolution of the ground state from antiferromagnetism to superconductivity

R. A. Fisher,[1] F. Bouquet,[1] N. E. Phillips,[1] M. F. Hundley,[2] P. G. Pagliuso,[2] J. L. Sarrao,[2] Z. Fisk,[3] and J. D. Thompson[2]
[1]*Lawrence Berkeley National Laboratory and Department of Chemistry, University of California, Berkeley, California 94720*
[2]*Los Alamos National Laboratory, Los Alamos, New Mexico 87545*
[3]*NHMFL, Florida State University, Tallahassee, Florida 32306*
(Received 1 April 2002; published 31 May 2002)

Resistivity measurements on $CeRhIn_5$ have suggested an unusual ''first-order-like'' transition from antiferromagnetism to superconductivity at a critical pressure P_c, ~15 kbar: At pressures below P_c the magnetic ordering temperature is approximately independent of pressure. At P_c antiferromagnetism disappears abruptly and is replaced by superconductivity, with a critical temperature that is also approximately independent of pressure. Here we report measurements of the low-temperature specific heat of $CeRhIn_5$ at pressures to 21 kbar, and for 21 kbar in magnetic fields to 70 kOe. They confirm, by measurement of a bulk thermodynamic property, the unusual relation between magnetism and superconductivity, and permit an estimate of the discontinuity in entropy at P_c. They also give insight into the natures of the antiferromagnetic and superconducting states and their changes with pressure: With increasing pressure the zero-field specific-heat anomaly changes from one typical of antiferromagnetic ordering at ambient pressure to one more characteristic of the formation of a Kondo singlet ground state at 21 kbar. The change in general shape of the anomaly is gradual, but at P_c, where the data suggest a weak thermodynamic first-order transition, there is a discontinuous change from an antiferromagnetic ground state to a superconducting ground state. Below P_c the quasiparticle density of states increases and the spin-wave stiffness decreases with increasing pressure. At P_c the low-energy magnetic excitations disappear and are replaced by excitations that are characteristic of superconductivity with line nodes in the energy gap. The quasiparticle density of states is continuous at P_c, but decreases with increasing pressure, to zero at 21 kbar. These features suggest the possibility of superconductivity with *d*-wave pairing and, at intermediate pressures, ''extended gaplessness.'' At 21 kbar except for the line nodes, the Fermi surface is fully gapped. The specific-heat data also show the existence of a second-order transition in the 11–12-kbar region, where features in the magnetic susceptibility and resistivity have been observed.

DOI: 10.1103/PhysRevB.65.224509 PACS number(s): 74.25.Bt, 74.70.Tx, 75.50.Ee, 75.40.Cx

The occurrence of superconducting (SC) heavy-fermion (HF) compounds provides a unique opportunity for investigating the relation between magnetism and superconductivity, particularly the possibility of magnetically mediated pairing of the electrons. In magnetic HF compounds there is a competition between magnetic order, driven by the Ruderman-Kittel-Kasuya-Yosida (RKKY) interaction, and the spin-singlet ground state, favored by the Kondo interaction.[1] Both interactions are governed by the local-moment–conduction-electron exchange $|J|$, but the dependence on $|J|$ is different, quadratic for the RKKY and exponential for the Kondo interaction. Since $\partial|J|/\partial P>0$, the application of pressure (P) can reduce the magnitude of the ordered magnetic moments and lower the ordering temperature. For appropriate values of the relevant parameters the Néel temperature (T_N) of an antiferomagnetic (AF) HF compound, and the Curie temperature (T_C) of a ferromagnetic (FM) HF compound can be driven to zero at a critical pressure (P_c). There has been considerable speculation that superconductivity might appear at that quantum critical point (QCP) with the electron pairing mediated by strong magnetic fluctuations, but the number of likely examples is small, presumably because the conditions that must be satisfied for superconductivity to be realized are so restrictive. Those conditions and the relevant concepts have been summarized in the context of the observed superconductivity in AF $CePd_2Si_2$ and $CeIn_3$, and a general phase diagram proposed.[2] The properties at AF and FM QCP's might be expected to be different, but, although the phase diagram for FM UGe_2 differs in detail from those for $CePd_2Si_2$ and $CeIn_3$,[3] it is remarkably similar in general form. For all three of these materials the critical temperature for magnetic ordering approaches zero at P_c, and superconductivity appears in a narrow window of P with a strongly P-dependent critical temperature (T_c), in accord with a model[2] in which a ''continuous'' transition at P_c is a condition for the occurrence of superconductivity. Antiferromagnetic $CeRhIn_5$, for which resistivity measurements have shown a phase diagram of a very different form,[4] presents a striking contrast with those materials and with theoretical considerations generally: T_N, ~4 K, is only weakly dependent on P to 14.5 kbar; at the next higher P, 16.3 kbar, the signature of AF order has disappeared and superconductivity, with an essentially P-independent T_c of ~2 K, appears. This phase diagram is qualitatively different from that of any other Ce HF compound, and, although the thermodynamic nature of the transition cannot be unequivocally determined from transport properties, the abrupt change at P_c suggests a ''first-order-like transition.''[4]

Measurements of the specific heat (C) can give information about the thermodynamic nature of the transition and low-T excitations relevant to an understanding of the relation between magnetism and superconductivity, information that

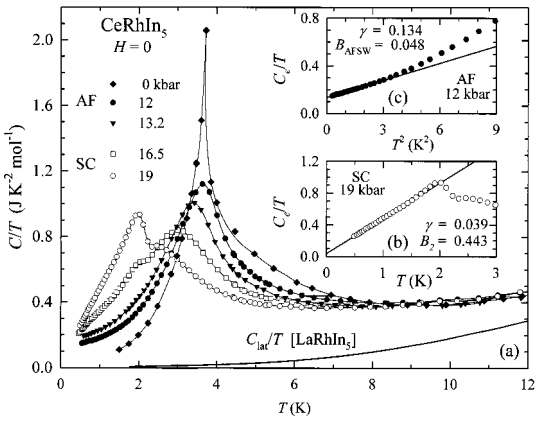

FIG. 1. (a) The specific heat, for representative values of P, as C/T vs T. The $P=0$ data are from Ref. 4. The insets show C_e in the low-T limit: (b) for $P>P_c$, and $C_e=\gamma T+B_2T^2$; and (c) for $P<P_c$, and $C_e=\gamma T+B_{\mathrm{AFSW}}T^3$.

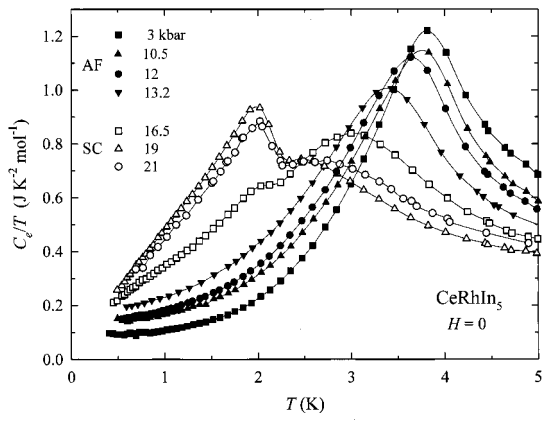

FIG. 2. C_e for $P\neq 0$. Data for 16 kbar are omitted for clarity.

is not obtained from the more usual measurements of resistivity and magnetization. The measurements reported here show that the superconductivity is a bulk property, and characterize its nature. They determine the quasiparticle density of states and the nature of the other low-energy excitations, thereby identifying the ground states throughout the range of P. The ground states, AF below P_c and HF/SC above, both evolve continuously with increasing P, but at P_c there is a discontinuous change: Long-range AF order disappears and superconductivity appears. Some of the low-T entropy associated with magnetic degrees of freedom at $P=0$ appears as entropy of typical HF-SC excitations at $P>P_c$. The data suggest, within the limits of resolution imposed by the discrete values of P, the occurrence of a weak thermodynamic first-order transition at P_c.

The sample, consisting of small, randomly oriented crystals, was contained in a clamped pressure cell with AgCl as the pressure-transmitting medium, and Sn and Pb manometers, one at each end of the sample. The pressure differences between the two ends of the sample were at most 0.2 kbar.

Zero-field measurements of C are shown in Fig. 1 for representative values of P. (In all figures, results associated with the AF phase are represented by solid symbols, with the SC phase by open symbols.) The lattice heat capacity (C_{lat}), taken to be the same as that of $LaRhIn_5$,[4] and shown in Fig. 1, was subtracted from C to obtain the ''electron'' contribution (C_e), shown on an expanded scale in Fig. 2. With increasing P the ''magnetic'' specific-heat anomaly, which is associated with AF ordering at ambient pressure, becomes broadened and reduced in amplitude. A second anomaly, associated with the transition to the SC state, first appears as a small irregularity at 16 kbar (in data that are too close to those at 16.5 kbar to be included in the figures). It grows to a ''shoulder'' on the magnetic anomaly at 16.5 kbar and reaches its maximum amplitude at 19 kbar. The data permit plausible extrapolations to $T=0$, and the entropy (S_e) calculated at 12 K has the same value for all P to within $\pm 2\%$.

Characteristic temperatures derived from C_e and ρ are compared in Fig. 3. The temperature of the maximum (T_{max}) of the magnetic anomaly in C_e/T tracks the T_N deduced from ρ (including the small increase at low P) for $P\leqslant 10$ kbar, but then shifts to lower T. (At 12 kbar T_N, determined by nuclear quadrupole resonance (NQR) measurements,[5] is close to T_{max}.) For $P\geqslant P_c$, T_{max} is close to the unidentified feature[4] in ρ at $T_?$. (Evidently measurements of ρ detect two features in the 9–15-kbar region that are not resolved in measurements of C_e.) Values of T_c, taken as the midpoints of entropy-conserving constructions on C_e/T (see, e.g., Fig. 4), are in good agreement with the values determined from ρ, which correspond to the onset of superconductivity.

For $P=21$ kbar and $H=0$, 50, and 70 kOe, the specific heat is shown in Fig. 4. The values of $T_c(H)$ obtained from the data do not extend to sufficiently high values of H to establish unambiguously the form of $H_{c2}(T)$ over a wide interval in T, but with the assumption of a parabolic T dependence they extrapolate to $H_{c2}(0)=159$ kOe (see Fig. 5) with a statistical uncertainty of $\sim$20 kOe. This value, which is in satisfactory agreement with the 152 kOe estimated from resistivity data,[4] far exceeds the Pauli limit,[6] $H_P(0)\approx 39$ kOe. For $T<T_c(H)$, $C_e(H)=\gamma(H)T+B_2(H)T^2$, and extrapolations to 0 K give the same S_e, 0.99 mJ K^{-1} mol^{-1}, at $T_c(0)$, 2.12 K, to within $\pm 1\%$. This dependence of C_e on T and H is characteristic of a certain group of heavy-fermion superconductors that includes, e.g., URu_2Si_2 (Ref. 7) and

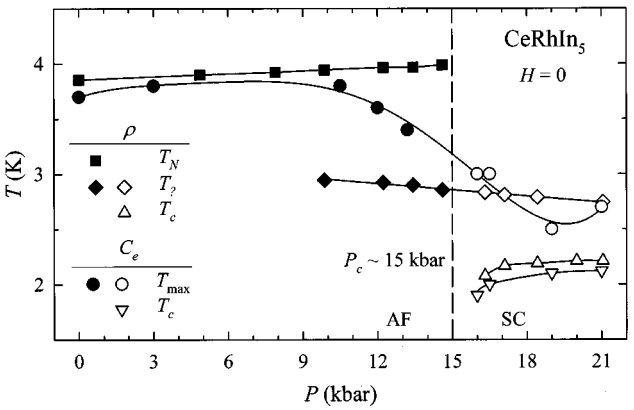

FIG. 3. Phase diagram for $CeRhIn_5$ constructed from C data and ρ data from Ref. 4 (see the text).

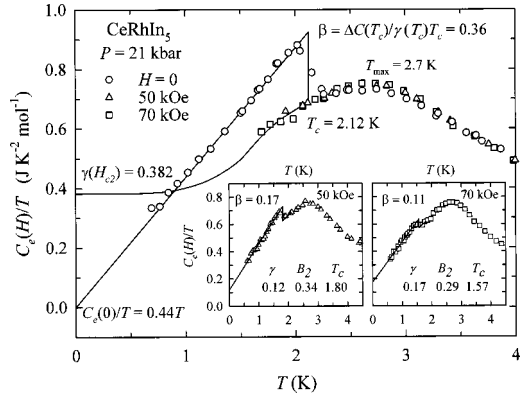

FIG. 4. $C_e(H)$ at 21 kbar Normal-, mixed-, and superconducting-state data for $C_e(H)$, with an extrapolation of the normal-state data to 0 K that is consistent with the superconducting-state entropy at T_c and the normal-state γ, $\gamma(H_{c2})$ or $\gamma'(0)$. The insets show $C_e(H)$ for 50 and 70 kOe.

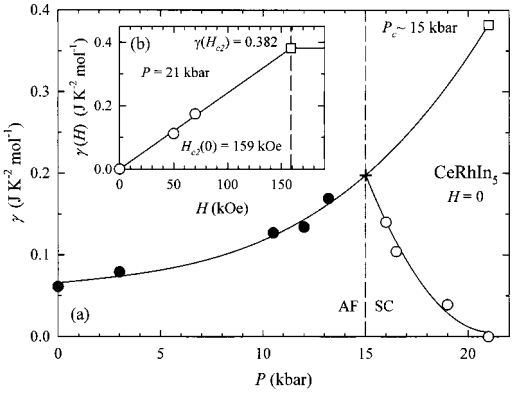

FIG. 6. (a) Zero-field values of γ vs P. (b) $\gamma(H)$ vs H for $P=21$ kbar. In (a) and (b) the open square is the 21-kbar, normal-state value of γ obtained by the extrapolation of the 0-, 50-, and 70-kOe values to $H_{c2}(0)=159$ kOe, represented in (b).

UPt_3.[8] The $B_2(0)T^2$ term is associated with line nodes in the energy gap and an ''unconventional'' order parameter.[9] Although line nodes can arise from extended *s*-wave pairing, they are commonly attributed to a *d*-wave order parameter in HF compounds.[9] The corresponding power-law T dependence for nuclear-spin-relaxation times[9] has been seen[6,10] in NQR measurements. For this pressure, and to within the experimental uncertainty,[11] $\gamma(0)=0$ and C_e in the superconducting state (C_{es}) is $C_{es}=B_2(0)T^2$. The value of $\gamma(0)$ shows that the Fermi surface (except for the line nodes) is fully gapped. For $T\leqslant T_c(H)$, $C_e(H)$ and $S_e(H)$ conform to expectations for superconducting material, and any additional contributions to C_e must be negligible. By that criterion, the superconductivity at 21 kbar is complete as well as bulk.

C_e in the normal state (C_{en}) is defined to within narrow limits at 21 kbar (see Fig. 4): For $T>T_c(H)$, C_{en} is independent of H and determined by the 70-kOe data to 1.7 K. In Fig. 6(b) it is shown that $\gamma(H)$ is approximately proportional to H, and extrapolation to $H_{c2}(0)$ gives $\gamma=382$ mJ K^{-2} mol^{-1} for the normal-state value, the 0-K intercept of C_{en}/T in Fig. 4. (For internal consistency the values of γ and some other parameters are given to more significant figures than warranted by the data.) The interpolation between 1.7 and 0 K must give the same $S_e(T_c)$ as that given by the data for $H=0$, 50, and 70 kOe. The curve in Fig. 5 is a smooth, plausible interpolation that satisfies this condition on the area under the curve. It is almost unique among such possibilities in the sense that any curve that is free of irregular peaks and dips and satisfies this constraint would have to be very similar. Its shape is similar to that of the Kondo singlet-ground-state ordering in some other HF compounds, e.g., URu_2Si_2 (Ref. 7) and $CeAl_3$,[12] and conspicuously different from that characteristic of AF ordering. Its H independence also suggests that the ''magnetic'' anomaly in C_e is not associated with AF ordering at this pressure.

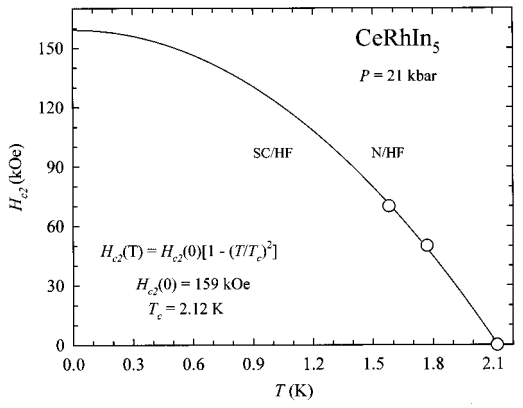

FIG. 5. $H_{c2}(T)$ vs T for $P=21$ kbar. The curve represents a parabolic fit to the data (see the text).

The discontinuity in C_e at T_c is relatively small: $\beta\equiv\Delta C_e(T_c)/C_{en}(T_c)=[C_{es}(T_c)-C_{en}(T_c)]/C_{en}(T_c)$ is 1.43 for a BCS superconductor and ~1 to 1.5 for a number of HF superconductors, but only 0.36 for $CeRhIn_5$. However, the small value is a direct consequence of the T dependence of C_{en}, the T dependence of C_{es}, and the thermodynamic requirement that the entropies of the superconducting and normal states be equal at T_c: $S_{es}(T_c)=S_{en}(T_c)=S_e(T_c)$. This requires no independent microscopic interpretation. If $C_{es}=B_2(0)T^2$ and $C_{en}=\gamma T$, with γ constant, the equality of entropies at T_c requires that $\beta=1$. For $CeRhIn_5$, as for many other HF superconductors, C_{en} does not correspond to a constant density of quasiparticle states, and must be represented by a T-dependent γ', defined by $C_{en}(T)\equiv\gamma'(T)T$. In this case, $\beta=B_2(0)T_c/\gamma'(T_c)-1$, which is 0.36 for $CeRhIn_5$, as observed. The value of $\gamma'(0)$ was determined independently, and the interpolation to the value of C_{en}/T to 1.7 K in Fig. 4 was drawn to satisfy the requirement that $S_{en}(T_c)=S_{es}(T_c)$. However, the thermodynamic argument can be turned around to show that the small value of β supports the derived value of $\gamma'(0)$ and the interpolation: The area under the curve for C_{en}/T has to be that shown in Fig. 4. $CeRhIn_5$ is evidently a somewhat extreme case in which γ' is still strongly T dependent at T_c, but it is not qualitatively different from, e.g., URu_2Si_2 for which the deviation of $\gamma'(T)$ from $\gamma'(T_c)$ is less precipitous and only 20% at 0 K, and $\beta\sim0.9$.[7]

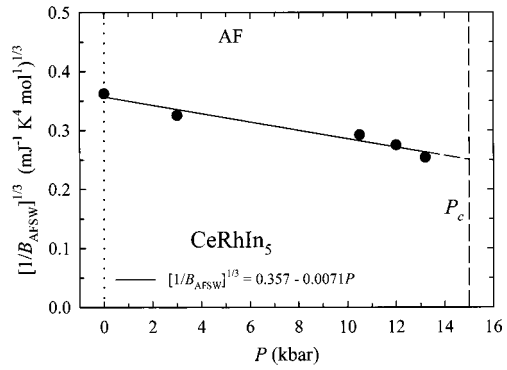

FIG. 7. The coefficient of the AF spin-wave term in C_e, B_{AFSW}, plotted as $(1/B_{\mathrm{AFSW}})^{1/3}$ vs P to demonstrate the linear-in-P decrease in the AF spin-wave stiffness (see the text).

Although the magnetic anomaly in C_e evolves with increasing P without a discernable discontinuity in its general shape, the T dependence of C_e at low T is discontinuous at P_c, as is apparent in Figs. 1(a) and 2, where C_e/T shows a positive curvature for $P<P_c$, but a zero curvature for $P>P_c$ as $T\rightarrow 0$. For all P, the lowest-order term in C_e is $\gamma(H)T$. For $P<P_c$, the second term is $B_{\mathrm{AFSW}}(H)T^3$ [Fig. 1(c)], which corresponds to the spin-wave (SW) contribution expected for an antiferromagnet; for $P>P_c$, it is $B_2(H)T^2$ [Fig. 1(b)], which is characteristic of certain heavy-fermion superconductors. With increasing P, $B_{\mathrm{AFSW}}(0)$ increases monotonically through the AF region, corresponding to a linear-in-P decrease in the spin-wave stiffness, which is proportional to the product of the moment and the exchange interaction. The decrease in spin-wave stiffness, represented in Fig. 7 as $(1/B_{\mathrm{AFSW}})^{1/3}$ vs P, amounts to 30% at 13.2 kbar. At P_c, $B_{\mathrm{AFSW}}(0)T^3$ is replaced by the superconductivity-related term $B_2(0)T^2$, the coefficient of which then increases monotonically to an approximately constant value at 19 kbar.[11] The four points in Fig. 8 do not characterize definitively the behavior of $B_2(0)$ over the range of P of interest, and their representation by two straight-line segments is somewhat arbitrary. The P dependence of $\gamma(0)$ is displayed in Fig. 6(a): The experimental AF values are interpolated to

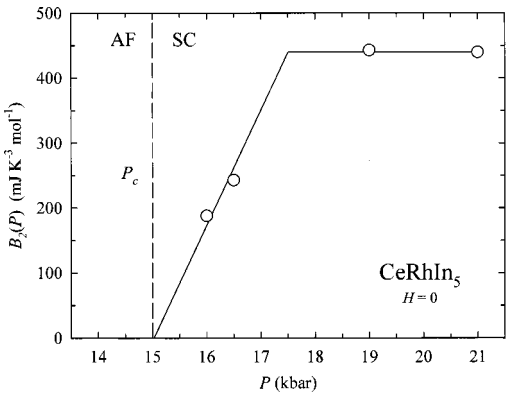

FIG. 8. $B_2(P)$ vs P. Above 19 kbar $B_2(P)$ is constant to within experimental uncertainty. The straight lines are arbitrary interpolations and extrapolations.

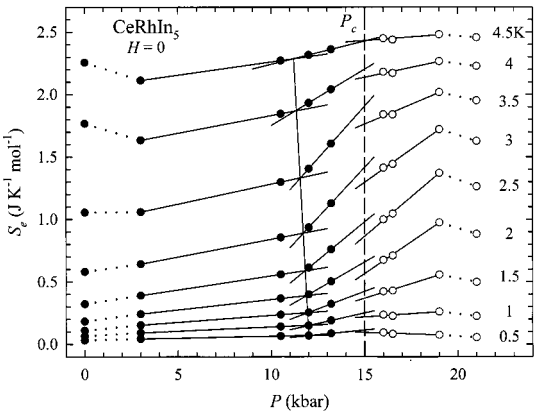

FIG. 9. Isotherms of $S_e(P)$ vs P showing features at 12 and 15 kbar which are emphasized by the straight-line approximations (see the text).

the 21-kbar normal-state value, which was derived from the mixed-state data; the experimental SC values are extrapolated to the AF curve at 15 kbar, the approximate value of P_c deduced from resistivity measurements.[4] The resulting curves represent a normal-state γ, which measures the density of low-energy quasiparticle excitations, that increases monotonically from ambient pressure to 21 kbar. In zero field and $P\geqslant P_c$, there is a transition to the superconducting state, but it leaves a ''residual'' $\gamma(0)$ that varies between the full normal-state value at P_c and zero at 21 kbar.

On the SC side of the phase boundary at P_c, $\gamma(0)$ is the same in the SC and normal states and $\Delta C_e(T_c)=0$. With increasing P, $\gamma(0)\rightarrow 0$ and $\Delta C_e(T_c)$ increases, but with essentially no increase in T_c. The extended gapless regions on the Fermi surface of superconductors with $d_{x^2-y^2}$ pairing[13] suggest a possible basis for understanding this behavior: Below a critical value of the pairing potential the gap vanishes and there is a finite density of low-energy quasiparticle states, $\gamma(0)\neq 0$. With increases in the pairing potential the gap appears and increases in amplitude, and the quasiparticle density of states decreases. For sufficiently high gap amplitudes the quasiparticle density of states approaches zero. The observed relation between $\Delta C_e(T_c)$ and $\gamma(0)$ would correspond to an increase in the gap amplitude and pairing potential with increasing P.

Isotherms, $S_e(P)$ vs P, obtained by integration of $C_e(T)/T$ to obtain $S_e(T)$ and interpolation to fixed T's, are shown in Fig. 9. They are related to the volume thermal expansion (α), which is proportional to $(\partial S_e/\partial P)_T$ in magnitude but opposite in sign. Although the isotherms show that α is negative in most of the range of P and T they are consistent with the positive values reported[14] at ambient pressure and temperatures above 1 K. The isotherms reveal interesting features near 12 and 15 kbar, which are emphasized in Fig. 9 by three straight-line segments that connect data points in limited intervals of pressure. The straight lines represent discontinuities, in $(\partial S_e/\partial P)_T$ near 12 kbar and in S_e at 15 kbar, which correspond, respectively, to second- and first-order thermodynamic transitions. For any one isotherm the features at 12 and 15 kbar, represented by the straight lines, are comparable in magnitude to the deviations of the points from

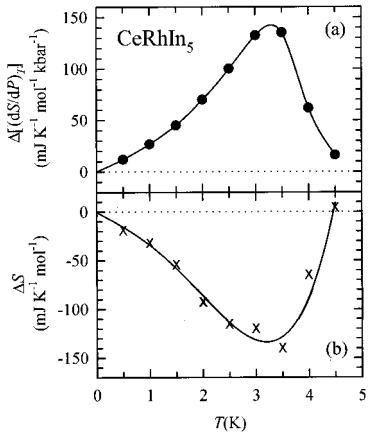

FIG. 10. The T dependence of the features represented by the straight-line approximations to the isotherms in Fig. 9. (a) $\Delta[(\partial S/\partial P)_T]$ vs P in the 11–12-kbar region, which corresponds to a second-order transition. (b) ΔS_e vs P at $P_c = 15$ kbar which corresponds to a weak first-order transition from the AF state to the SC state.

a smooth curve that might be drawn as an approximate fit to all the points. However, both their systematic variations from one isotherm to the next, which are shown in Fig. 10, and their relation to other properties (see below) attest the reality of structure at least qualitatively similar to that represented by the lines. Furthermore, both discontinuities extrapolate to zero at $T=0$, as required by the third law of thermodynamics, and both tend to small numerical values at temperatures above that of the magnetic ordering, as might be expected if they were associated with the magnetic ordering. The striking similarity of the temperature dependence of $\Delta(\partial S_e/\partial P)_T$ to that of ΔS_e suggests a more direct relation between the two transitions than might be expected for a common origin in the magnetic properties alone, but there is no obvious independent evidence of that.

The feature near 12 kbar, the better defined of the two, is a discontinuity in $(\partial S_e/\partial P)_T$, which corresponds to a discontinuous increase in the magnitude of α, which is negative, and a second-order transition. The phase boundary, represented by the nearly vertical solid line in Fig. 9, is defined by the intersections of the straight-line segments of the isotherms, which occur at 12.0 and 11.2 kbar at 0.5 and 4.5 K, respectively. This is a region of the phase diagram in which features in the resistivity and susceptibility have been observed,[4] and also where $T_{\max}$ starts to deviate from its low-P value (see Fig. 3). With the slope of the phase boundary and the Ehrenfest relation, the maximum value of $\Delta(\partial S_e/\partial P)_T$ gives a maximum discontinuity in C of ~ 50 mJ K^{-1} mol^{-1}. The experimental data do not permit a meaningful quantitative comparison, but they are not inconsistent with that value.

The feature at 15 kbar is less well defined, but the points above and below 15 kbar cannot be connected by smooth curves without a change in sign of the curvature. The vertical dashed line in Fig. 9 represents a phase boundary at $P_c = 15$ kbar, as defined by the construction in Fig. 6, and taken to be independent of T. The straight-line representations of the isotherms then correspond to a finite ΔS_e at P_c, and a first-order transition from a low-P phase, which must have the larger volume, to a high-P phase that has a lower S_e. The values of $-\Delta S_e$ reach a maximum, ~ 0.13 J K^{-1} mol^{-1} $= 0.022R \ln 2$, near 3 K, and extrapolate to zero near 4.5 K. At 1 K and below, they correspond, to within a factor 2, to the extrapolations to P_c of the low-T terms in C_e depicted in Figs. 6, 7, and 8. The vertical phase boundary drawn in Fig. 3 would imply a zero change in volume at P_c; a slope of 2 K kbar^{-1} would correspond to a maximum fractional change in volume of $\sim 3\times 10^{-5}$. This interpretation of the isotherms corresponds to a transition from the AF state to the SC state that includes a small first-order component, which terminates at a critical point in the vicinity of the magnetic ordering temperature. This is supported by its consistency with other properties of the system, as well as by the systematic variation with T of the values of ΔS_e obtained by the straight-line constructions in Fig. 9. The plausibility of this interpretation of the isotherms notwithstanding, it must be recognized that the points on the isotherms are not sufficiently closely spaced in P to define precisely the interval in which ΔS_e occurs. The data do not distinguish between a ''sharp'' transition that takes place in a few tenths of a kilobar, a width that might be attributed to sample and pressure inhomogeneities, and a broader feature in S_e that is not a thermodynamic phase transition. In the latter case the values of ΔS_e would be measures of the discrepancies between the values of S_e at P_c obtained by extrapolations from higher and lower pressures. However, as such, they would still be relevant to understanding the ''transition.'' Furthermore, they would put an upper limit to the entropy discontinuity accompanying any ''real'' first-order transition.

We are grateful to A. V. Balatsky and V. Z. Kresin for helpful discussions. The work at LBNL was supported by the Director, Office of Basic Energy Sciences, Materials Sciences Division of the U.S. DOE under Contract No. DE-AC03-76SF00098. The work at LANL was performed under the auspices of the U.S. DOE. Z.F. acknowledges support through NSF Grant Nos. DMR-9870034 and DMR-9971348.

[1] S. Doniach, in *Valence Instabilities and Related Narrow Band Phenomena*, edited by R. D. Parks (Plenum, New York, 1977), p. 169.

[2] N. D. Mathur, F. M. Grosche, S. R. Julian, I. R. Walder, D. M. Freye, R. K. W. Haselwimmer, and G. G. Lonzarich, Nature (London) **394**, 39 (1998).

[3] S. S. Saxena, P. Agarwal, K. Ahilan, F. M. Grosche, R. K. W. Haselwimmer, M. J. Steiner, E. Pugh, I. R. Walker, S. R. Julian,

P. Monthoux, G. G. Lonzarich, A. Huxley, I. Sheikin, D. Braithwaite, and J. Flouquet, Nature (London) **406**, 587 (2000).
[4] H. Hegger, C. Petrovic, E. G. Moshopoulou, M. F. Hundley, J. L. Sarrao, Z. Fisk, and J. D. Thompson, Phys. Rev. Lett. **84**, 4986 (2000).
[5] T. Mito, S. Kawasaki, G.-Q. Zheng, Y. Kawasaki, K. Ishida, Y. Kitaoka, D. Aoki, Y. Haga, and Y. Onuki, Phys. Rev. B **63**, 220507(R) (2001).
[6] A. M. Clogston, Phys. Rev. Lett. **9**, 2669 (1962).
[7] R. A. Fisher, S. Kim, Y. Wu, N. E. Phillips, M. W. McElfresh, M. S. Torikachvili, and M. B. Maple, Physica B **163**, 419 (1990).
[8] R. A. Fisher, S. Kim, B. F. Woodfield, N. E. Phillips, L. Taillefer, K. Hasselbach, J. Flouquet, A. L. Giorgi, and J. L. Smith, Phys. Rev. Lett. **62**, 1411 (1989).
[9] R. H. Heffner and M. R. Norman, Comments Condens. Matter Phys. **17**, 325 (1996).
[10] Y. Kohori, Y. Yamato, Y. Iwamoto, and T. Kohara, Eur. Phys. J. B **18**, 601 (2000).
[11] A fit to all of the 21-kbar points at or below the maximum in C/T gives $\gamma(0)=5.4(11)$ mJ K^{-2} mol^{-1} and $B_2(0)=436(7)$ mJ K^{-3} mol^{-1}; with omission of the lowest point, which is conspicuously high, $\gamma(0)=-0.2(11)$ and $B_2(0)=440(7)$ mJ K^{-3} mol^{-1}. For comparison, the fit to the more precise 19-kbar data, below 1.6 K, gives $\gamma(0)=39(3)$ mJ K^{-2} mol^{-1} and $B_2(0)=443(3)$ mJ K^{-3} mol^{-1}.
[12] G. E. Brodale, R. A. Fisher, N. E. Phillips, J. Flouquet, and C. Marcenat, J. Magn. Magn. Mater. **54–57**, 419 (1986).
[13] S. Haas, A. V. Balatsky, M. Sigrist, and T. M. Rice, Phys. Rev. B **56**, 5108 (1997).
[14] T. Takeuchi, T. Inoue, K. Sugiyama, D. Aoki, Y. Tokiwa, Y. Haga, K. Kindo, and Y. Onuki, J. Phys. Soc. Jpn. **70**, 877 (2001).